Published in final edited form as:
Atherosclerosis. 2011 November ; 219(1): 151–157. doi:10.1016/j.atherosclerosis.2011.06.049.

Influence of Pericoronary Adipose Tissue on Local Coronary Atherosclerosis as Assessed by a Novel MDCT Volumetric Method

Pál Maurovich-Horvat, MD[a,b,*], **Kimberly Kallianos, BS**[a,*], **Leif-Christopher Engel, MD**[a], **Jackie Szymonifka, MA**[c], **Caroline S. Fox, MD MPH**[d], **Udo Hoffmann, MD, MPH**[a], and **Quynh A. Truong, MD, MPH**[a]

[a]Cardiac MR PET CT Program, Division of Cardiology and Department of Radiology, Massachusetts General Hospital, Harvard Medical School, Boston, Massachusetts

[b]Heart Center, Semmelweis University, Budapest, Hungary

[c]Department of Biostatistics, Massachusetts General Hospital, Harvard Medical School, Boston, Massachusetts

[d]National Heart, Lung, and Blood Institute's Framingham Heart Study, Framingham, MA

Abstract

Objective—Pericoronary adipose tissue (PCAT) may create a pro-inflammatory state, contributing to the development of coronary artery disease (CAD). We sought to evaluate the feasibility of avolumetric PCAT quantification method using a novel threshold based computed tomography approach. In addition we determined the relation between PCAT volumes and CAD.

Methods—In 51 patients (49.5±5.1 years, 64.8% male) who underwent 64-slice MDCT, we measured threshold-based PCAT volumes using distance and anatomic-based methods. Using the most reproducible method, we performed the proximal 40-mm distance measurement in three groups as stratified by coronary plaque and high-sensitivity C-reactive protein (hs-CRP) levels: Group 1 (presence of coronary plaque, hs-CRP >2.0 mg/L); an intermediate group (Group 2, no plaque, hs-CRP >2.0 mg/L); and Group 3 (no plaque, hs-CRP<1.0 mg/L). We compared PCAT volumes to the presence of coronary plaque on a patient (n=51) and vessel (n=153) basis. On a subsegment basis (n=1224), we compared PCAT volume to the presence of plaque as well as plaque morphology.

Results—Distance-based PCAT volume measurements yielded excellent reproducibility with intra-observer intraclass correlation (ICC) of 0.997 and inter-observer ICC of 0.951. On a both a per-patient and per-vessel analysis, adjusted PCAT volume was greater in patients with plaque (Group 1) than without plaque (Group 2 and 3, p<0.001). No difference in PCAT volume was seen between high and low hs-CRP groups without plaque (p=0.51). Adjusted PCAT volumes were

Address for Correspondence: Quynh A. Truong, MD MPH, Cardiac MR PET CT Program, Massachusetts General Hospital, 165 Cambridge Street, Suite 400, Boston, MA 02114, qtruong@partners.org, (telephone) 617-726-0798, (fax) 617-724-4152.
*Both authors contributed equally to this work.

Disclosures
No conflicts of interest to be disclosed.

higher in subsegments with plaque as compared without (p<0.001). Additionally, adjusted PCAT volume was greatest in subsegments with mixed plaque followed by non-calcified plaque, calcified plaque, and the lowest volume in segments with no plaque (p<0.001).

Conclusion—In this proof-of-concept study, threshold based PCAT volume assessment is feasible and highly reproducible. PCAT volume is increased in patients and vessels with coronary plaques. Surrounding vessel subsegments with coronary plaque, particularly mixed plaques, have greatest PCAT volume and highlight the effect of local PCAT in the development of coronary atherosclerosis.

Keywords

Coronary artery disease; pericoronary fat; epicardial fat; adipose tissue; inflammation; computed tomography

1. Introduction

Pericardial adipose tissue has been suggested to contribute to the development of coronary artery disease (CAD)(1–3). Pericoronary adipose tissue (PCAT) is part of the epicardial adipose tissue that directly surrounds the coronary arteries. It has been suggested that adipocytokines produced by PCAT might amplify vascular inflammation through paracrine effects, leading to local atherogenesis, plaque instability, and neovascularization (4–6). Few studies have examined the association between regional PCAT and atherosclerosis in the underlying coronary arteries (5,7–9). However, all of these studies utilized fat quantification techniques that were based on manual delineation of PCAT on the original axial slices.

In addition to local inflammatory processes, systemic inflammation as measured by high sensitivity C-reactive protein (hs-CRP) has been established as an independent risk factor for CAD (10). Several large clinical trials have demonstrated that patients with hs-CRP levels greater than 2 mg/L have less favorable clinical outcomes (11–13). In contrast, patients with levels of hs-CRP less than 1 mg/L have low cardiovascular risk according to a statement issued by the American Heart Association and Centers for Disease Control (14).

Cardiac computed tomography (CT) allows for simultaneous assessment of PCAT volume and coronary artery plaque. Volumetric quantification of PCAT in patients with and without CAD in conjunction with high and low hs-CRP levels could provide insights into the pathophysiological role of this distinct adipose tissue depot and its local effect on coronary atherosclerosis. Thus, we aimed to first assess the feasibility and reproducibility of a threshold-based method of PCAT volume quantification using cardiac CT and determine the relationship of PCAT volume to the presence of coronary atherosclerotic plaque and hs-CRP levels on per-patient and per-vessel basis. We also sought to determine whether the effect of coronary atherosclerosis is driven by local factors by examining the PCAT volume surrounding subsegments with plaque versus no plaque, as well as plaque morphology.

2. Methods

2.1. Study population

From May 2005 to May 2007 consecutive subjects were prospectively enrolled as part of the ROMICAT (Rule Out Myocardial Infarction using Computer Assisted Tomography) trial. Details of the study have been previously reported (15). From the 368 ROMICAT patients, we stratified based on presence of coronary atherosclerosis and hs-CRP levels in order to maximize the risk profile difference between the patient groups in this proof-of-concept study. We defined high hs-CRP as >2.0 mg/L and low hs-CRP as <1.0 mg/L, based on data

from recent clinical trials and scientific statements (11,12,16). In this age- and gender-matched 1:1:1 case-control design, we categorized patients into 3 groups: Group 1 (patients with coronary plaque and high hs-CRP); Group 2 (patients with no plaque and high hs-CRP), and Group 3 (patients with no plaque and low hs-CRP). After excluding 32 patients with left coronary artery dominance and 3 patients due to missing datasets, we identified a case group that included 49 patients with plaque and high hs-CRP (Group 1), of which we excluded 21 patients due to high image noise or artifacts. We then matched an intermediate group (Group 2) and the control group (Group 3) to age and gender, which resulted in the final cohort of 51 patients (17 patients in each group). Due to the insufficient number for the age- and gender-match (n=10), we were unable to include a 4^{th} group of patients with plaque and low hs-CRP.

2.2. Computed tomography imaging protocol

Contrast-enhanced gated CT imaging was performed using a standard coronary artery 64-slice MDCT (Sensation 64, Siemens Medical Solutions, Forchheim, Germany) imaging protocol that included the administration of 0.6 mg sublingual nitroglycerin in the absence of contraindications and 5–20 mg of intravenous metoprolol if the baseline heart rate was above 60 beats per minute. Images were acquired during a single inspiratory breath hold in spiral mode with 330 ms rotation time, 32 × 0.6 mm collimation, tube voltage of 120 kVp, maximum effective tube current-time product of 850 mAs, and tube modulation when possible. On average, 80 mL of iodinated contrast agent (Iodixanol 320 g/cm^3, Visipaque, General Electrics Healthcare, Princeton, NJ), followed by 40 mL saline solution was injected at a rate of 5 mL/s. A test bolus scan with 20 mL iodinated contrast followed by 40 mL saline at 5ml/s was used to calculate the beginning of image acquisition according to contrast agent transit time. Trans-axial data sets were reconstructed at 65% phase, with an image matrix of 512×512 pixels, a slice thickness of 0.75 mm, and an increment of 0.4 mm. All image analyses were performed offline on dedicated cardiac workstations.

2.3. Pericoronary adipose tissue volumetric assessment

Two independent readers who were blinded to the coronary plaque and hs-CRP results performed the PCAT reproducibility measurements using four distinct 3D-threshold based methods. For inter-observer reproducibility, Observer 1 and Observer 2 performed the measurements in 10 randomly selected patients. For intra-observer reproducibility, Observer 1 performed the measurements in these patients twice, one month apart. The reproducibility results are shown in Table 2.

After performing the reproducibility analysis, the proximal 40mm distance method of PCAT volume quantification technique was selected for further assessment as this method had the best reproducibility (Table 2). Using the proximal 40mm vessel distance method, one observer measured PCAT volume in all 51 patients, with a total of 153 vessels and 1224 coronary artery subsegments evaluated across the three patient groups.

2.3.1. Proximal 40 mm distance—The method of threshold-based volumetric PCAT assessment is based on a modified application of software for volumetric assessment of coronary atherosclerotic plaques (SUREPlaque, Vitrea 2, Version 3.9.0.1, Vital Images Inc, Plymouth, MN). Manual tracing was used to circle the region containing PCAT in cross-sectional images perpendicular to the vessel centerline in every 5 mm. The exact pericoronary fat volume within the manually traced region was calculated by the software using Hounsfield unit (HU) based thresholds (Figure 1). Voxels with values between the minimum setting of the SUREPlaque tool ((−149HU) and an upper threshold (−30HU) were determined to represent adipose tissue, and the total PCAT volume was calculated by summing these voxels along the course of each coronary artery. We recorded PCAT

volumes in 5 mm increments (subsegments), and summed PCAT along the measured vessel lengths. Voxels representing air, myocardium, or contrast enhanced blood pool in the selected region were excluded by the HU cutoffs.

2.3.2. Entire vessel length—For this method, PCAT volume was quantified surrounding the entire left anterior descending coronary artery (LAD), left circumflex coronary artery (LCx), and right coronary artery (RCA) extending to the distal portion of the vessel. We defined the distal vessel portion with a luminal diameter less than or equal to 2 mm.

2.3.3. Proximal anatomical segments—PCAT volume was also quantified in an anatomical segment-based method. The borders of the anatomical segments were established by the readers according to the recommendations of the American Heart Association(17). Using this method, PCAT quantification included the proximal first coronary segments (segment 1 of the RCA, segments 5 and 6 of the left main coronary artery (LM)/LAD, and segment 11 of the LCx).

2.3.4. Proximal two anatomical segments—Anatomical segment based measures were also performed in the proximal first-two coronary segments including segments 1 and 2 of the RCA, segments 5,6, and 7 of the LM/LAD, and segments 11 and 13 of the LCx.

2.4. Coronary Artery Plaque Assessment

The coronary plaque assessment was performed by one experienced CT reader who was blinded to the PCAT volume and hs-CRP results. To determine the exact anatomic location of coronary plaques, the first 40mm of the LM/LAD, LCx, and the RCA were evaluated using axial images, multiplanar reconstructions, thin-slab maximum intensity projections, and curved multiplanar reformatted images. The presence and morphology of coronary plaque was evaluated in 5mm subsegments of each vessel: 0–5mm, 5–10mm, 10–15mm, 15–20mm, 20–25mm, 25–30mm, 30–35mm, and 35–40mm positions from the ostium. Details on plaque detection and characterization have been previously described and validated.(15,18) Briefly, segments were defined as having calcified plaque, if a structure with a density of greater than 130 Hounsfield units (HU) could be visualized separately from the contrast-enhanced coronary lumen (because its density was above the contrast-enhanced lumen), be assigned to the coronary artery wall, and be identified in at least 2 independent planes. Non-calcified plaque was defined as any clearly discernible structure that could be assigned to the coronary artery wall in at least 2 independent image planes and had a CT density less than 130 HU units but greater than the surrounding connective tissue. Mixed coronary atherosclerotic plaque was defined as the presence of calcified and non-calcified plaque components within any single coronary artery segment.

2.5. Hs-CRP assessment

Blood samples from the peripheral vein were collected in an EDTA-coated tube within one hour prior to the coronary CT angiography scan. The samples were immediately centrifuged with the plasma aliquoted and stored at −80°C until analysis. Concentrations of hs-CRP were measured nephelometrically on a BN II analyzer (Dade-Behring, Marburg, Germany). Inter-assay coefficients of variation were <5% for nephelometry. Hs-CRP levels were defined as high if >2.0 mg/L and low if <1.0 mg/L, as described above.

2.6. Statistical analysis

Continuous variables are reported as mean ± standard deviation (SD) or median and interquartile range (IQR), as appropriate. Discrete variables are given in frequency and percentiles. To compare the differences in characteristics between the three groups, we used

analysis of variance (ANOVA) or Kruskal-Wallis test for continuous variables as appropriate and Fisher's Exact test for categorical variables. For reproducibility of PCAT volumes, we used the intraclass correlation coefficient (ICC) for intra-observer and inter-observer agreement and paired t-test for determining the significance of the mean absolute differences. In addition, inter-observer measures were assessed using the Pearson's correlation coefficient and a Bland-Altman graph. On a per-patient basis, the differences in PCAT volumes (both overall and within individual vessels) between the 3 groups were determined by employing mixed effects models with adjustment for body mass index (BMI), hypertension, hyperlipidemia. These covariates were chosen based on univariate analyses with p-value <0.10. This mixed model also allowed us to account for the matching that was performed. We also used mixed effects models for pairwise comparisons. For these models, we used parametric statistics for comparisons of the normally distributed PCAT volumes, with the exception of overall LAD where we used a non-parametric model due to its skewness. We performed a similar analysis with adjustment for vessel, distance, BMI, hypertension, hyperlipidemia, and CRP on a per-subsegment basis and compared segments with plaque versus no plaque, in addition to comparisons of plaque morphology. For mixed models, we report the mean ± standard error. A two-tailed p-value of <0.05 was considered significant. All analyses were performed using the SAS software (Version 9.2, SAS Institute Inc) and SPSS 16.0 (Chicago, Illinois).

3. Results

The baseline characteristics of the 51 patients as stratified by the 3 groups are described in Table 1. Overall, traditional risk factors were most prevalent in Group 1. Notably, hyperlipidemia was more frequent in Group 1 patients (plaque, hs-CRP>2 mg/L) compared to patients in Group 2 (no plaque, hs-CRP>2 mg/L) or Group 3 (no plaque, hs-CRP<1 mg/L) (p=0.01). BMI varied across the three studied groups, with the greatest BMI measured in Group 2 patients (no plaque, hs-CRP>2) (p=0.05). Additionally, the proportion of patients with hypertension trended to be decreased across the groups (p=0.09).

3.1. Reproducibility of PCAT volumes

The reproducibility of the entire vessel based, the segment based and the proximal 40 mm based PCAT assessments was compared. The proximal 40 mm vessel assessment yielded the highest ICC value (Table 2), with an excellent intra-observer ICC 0.997 and inter-observer ICC of 0.951 overall. In contrast, the per-patient entire vessel based inter-observer ICC was 0.405 and the anatomical segment based ICC was a modest 0.802 for one proximal coronary segment and 0.670 for two proximal coronary segments. The modest intra- and inter-observer variability of the anatomical segment based analysis was essentially due to the poor reproducibility of the LCx assessment. The course of the vessel varies greatly, as often a large obtuse marginal branch gives the outflow tract and the remaining LCx is a small vessel. Thus, depending on the observer's adjudication, the assessed vessel portion might have differed significantly. Therefore, we performed all our subsequent analysis using the 40 mm distance based approach as this minimized the variability in segment selection and allowed both observers to measure a standardized length of vessel. Supplementary appendix 1 depicts Bland-Altman analysis of the individual reads by Observer 1 and 2 for the proximal 40mm PCAT volume on a patient basis with good concordance and no systematic bias.

3.2. Patient based analysis

The average PCAT volume surrounding the proximal 40 mm of the coronary arteries was 26.98±13.33 cm^3 (range: 5.45 – 60.54 cm^3). In a patient-based analysis (Table 3), PCAT volume differed significantly across the three groups (p<0.001), and was greater in patients

with coronary plaque (Group 1) than no plaque irrespective of hs-CRP levels (Group 2: high hs-CRP, $p<0.001$) and (Group 3: low hs-CRP, $p<0.001$). Moreover, in patients without plaque, no difference in PCAT volume was seen between patients with high and low hs-CRP levels ($p=0.514$). The difference in PCAT volumes remained significant across the three patient groups after adjustment for BMI, hypertension, and hyperlipidemia.

3.3. Proximal 40 mm vessel-based analysis

The proximal 40 mm vessel-based analysis of PCAT was performed in 153 vessels including 51 left anterior descending, 51 left circumflex, and 51 right coronary arteries. Similar to the patient-based analysis, a significant difference in PCAT volume was observed among the groups in all three vessel territories (Table 3). Adjusted mean PCAT volume was greatest surrounding the right coronary artery.

3.4. Subsegment based analysis in subsegments with and without plaque

Figure 2 and Supplementary Appendix 2 shows the relationship of local adipose tissue volume and presence of adjacent coronary plaque. A subsegment-based analysis was performed in 5 mm increments to assess PCAT quantity adjacent to 1224 vessel subsegments with and without plaque. No atherosclerotic plaque was detected in 1005 subsegments while 219 subsegments contained plaque. The mean fat volume surrounding 5 mm vessel subsegments with plaque was higher compared to subsegments without plaque ($p<0.001$) when adjusting for patient, vessel, distance from the ostium, as well as BMI, hypertension, hyperlipidemia, and hs-CRP. In addition, the adjusted mean PCAT volume was greater in subsegments with plaque than segments without plaque when analyzed for each coronary vessel separately (all $p<0.001$) with the exception of the LCx ($p=0.14$).

3.5. Subsegment based analysis comparing plaque morphology

An analysis of the relationship between PCAT volume and plaque type was performed which demonstrated that there is a gradient effect with higher PCAT volume surrounding segments with mixed plaque followed by non-calcified plaque, calcified plaque, and the lowest volume in segments with no plaque ($p<0.001$) (Figure 3). While there is no difference between calcified plaque and no plaque ($p=0.12$), we did find a difference between mixed plaque and non-calcified plaque as compared to no plaque (both $p\leq0.01$). When comparing amongst plaque types, PCAT volume was greater surrounding segments with mixed plaque as compared to calcified plaque ($p=0.04$); no significant difference was seen when comparing the other plaque morphologies (all $p>0.1$).

4. Discussion

We describe a threshold based three-dimensional (3D) quantification method to assess PCAT volume around the proximal 40 mm of the coronary arteries. This threshold-based method is similar to techniques used for coronary artery plaque quantification and characterization (19,20). Our technique allows for adipose tissue assessment along the course of the coronary artery through the generation of a three-dimensional color-coded map of voxels containing adipose tissue. The volumetric quantification of the adipose tissue compartment is achieved by summing voxels within the predefined HU range. The strength of our method is that it allows volumetric assessment around all three main epicardial coronary arteries, and a detailed analysis of short PCAT subsegments and their relation to underlying coronary atherosclerotic plaque. Furthermore, it has an excellent intra- and inter-observer reproducibility, which is in line with several other studies utilizing volumetric measurements for adipose tissue quantification in different body regions (2,5,9,21,22).

The most commonly used techniques for PCAT quantification in cardiac CT datasets are based on two-dimensional (2D) measurements of thickness and area, both of which are measured using a limited number of axial slices (5,7,8,23). The reproducibilities of 2D metrics have been modest, with coefficient of variation between 12.0% – 23.4% and inter-observer ICC of 0.76 (95% CI 0.50 – 0.88) (5,7,8). Moreover, these 2D quantification techniques may not account for the inhomogeneous distribution of PCAT along the atrioventricular and interventricular grooves due to the limitations posed by the single CT cross-sectional assessment. These limitations could explain the conflicting data on the association of PCAT thickness and coronary atherosclerosis (7,8).

A recently published PCAT quantification method by Mahabadi et al relies on tracing and summing PCAT areas in the transaxial slices (9). Furthermore, another important difference is that Mahabadi et al excluded PCAT surrounding the RCA due to limitations of the method they used (9). We included only patients with right coronary artery (RCA) dominance or co-dominance to avoid potential bias due to small RCA in coronary systems with left dominance. Notably we found that the quantification of the RCA territory actually yielded the highest PCAT volumes.

Our results indicate that elevated PCAT volume is related to plaque presence on a patient and vessel based evaluation in the LAD, LCx, and RCA vessel territories. These observations contribute to the increasing body of evidence that there is an association between PCAT and coronary artery disease (5,7–9). We believe it is important to quantify PCAT volumes at the subsegmental level to assess the relationship between plaque and directly adjacent adipose tissue. We found that PCAT volume is increased surrounding coronary subsegments containing plaque, which suggests a local effect of PCAT on coronary plaque development. Interestingly, PCAT volume was greatest in subsegments with mixed plaque followed by non-calcified plaque, calcified plaque, and the lowest volume in segments with no plaque. This suggests that perhaps while non-calcified plaque is part of the earlier stage of atherosclerosis and calcified plaque is part of the later chronic phase, the most active process is with the development of mixed plaques.

Furthermore, we stratified the cohort according to hs-CRP levels and presence of plaque in order to assess the systemic effects of inflammation on the relationship between PCAT volume and coronary artery disease. We found that patients without plaque had similar PCAT volumes despite differences in hs-CRP levels. These findings are in line with previous studies suggesting local processes in addition to systemic effects in the development of coronary atherosclerosis (4,6,7). Mechanistically, adipocytokines secreted by the pericoronary adipose tissue may diffuse into the vasculature and lead to the development of atherosclerotic changes in the adjacent vessel wall via local inflammatory effects, thus plasma inflammatory markers may not adequately reflect local tissue inflammation and atherogenesis (6). Further larger studies are needed to examine the effect of local adipocytokines on atherosclerotic plaque development.

4.1. Study Limitations

There are several limitations to the current study. Since our case-control matching was performed within the ROMICAT cohort, we did not include analysis on a fourth group (patients with coronary plaque but low hs-CRP levels) due to inadequate number of patients for age- and gender-matching. The results of this small feasibility study require validation in a larger dataset and may allow for sufficient number to examine this interesting fourth group. We have used fixed 40mm proximal-distal measurements due to its high reproducibility. Moreover, it is important to note that most of plaque ruptures occur in the proximal 40 mm region of the coronary arteries (20). Our findings may not be applicable to distal vessels beyond 40 mm or left-dominant coronary systems. In addition, the LM was

counted towards the LAD, thus the proportion of the investigated LAD might be relatively smaller than for RCA and LCx. However, this should not affect the feasibility and reproducibility of the quantification method. Since the measurement software used to assess PCAT was dedicated to coronary plaque evaluation with a limited range of HU settings, therefore the lower limit of the HU value for fat quantification was defined by the lowest selectable HU value (−149 HU) in the software application. Furthermore, due to the partial overlap of the quantified adipose tissue volumes around at left main stem bifurcation, we may be double sampling the fat containing voxels in some of the proximal LAD and LCx subsegments. These limitations could be addressed by the future development of dedicated software for PCAT volume assessment.

5. Conclusion

In this proof-of-concept study, we demonstrate the feasibility and excellent reproducibility of a novel threshold-based method for PCAT volume assessment. The local amount of PCAT volume was increased in patients and vessels with coronary plaques. In patients without plaque, PCAT volume did not differ based on hs-CRP level. Surrounding vessel subsegments with coronary plaque, particularly mixed plaques, have greatest PCAT volume. These findings suggest that coronary atherosclerosis may be mediated by local effect of PCAT in addition to systemic inflammatory processes. Further studies are needed to validate our findings and elucidate the role of local adipocytokines on atherosclerosis.

Supplementary Material

Refer to Web version on PubMed Central for supplementary material.

Acknowledgments

We would like to thank Hang Lee, PhD for his statistical guidance.

Sources of Funding

This work was supported by the NIH R01 HL080053, and in part supported by Siemens Medical Solutions and General Electrics Healthcare. Dr. Truong received support from NIH grant K23HL098370 and L30HL093896. Dr. Maurovich-Horvat received support from TAMOP-4.2.2-08/01/KMR-2008-2004.

Abbreviation list

BMI	body mass index
CAD	coronary artery disease
CT	computed tomography
Hs-CRP	high-sensitivity C-reactive protein
LAD	left anterior descending artery
LCx	left circumflex coronary artery
LM	left main coronary artery
PCAT	pericoronary adipose tissue
RCA	right coronary artery
ROMICAT	Rule Out Myocardial Infarction using Computer Assisted Tomography

References

1. Rosito GA, Massaro JM, Hoffmann U, et al. Pericardial fat, visceral abdominal fat, cardiovascular disease risk factors, and vascular calcification in a community-based sample: the Framingham Heart Study. Circulation. 2008; 117:605–13. [PubMed: 18212276]
2. Mahabadi AA, Massaro JM, Rosito GA, et al. Association of pericardial fat, intrathoracic fat, and visceral abdominal fat with cardiovascular disease burden: the Framingham Heart Study. Eur Heart J. 2009; 30:850–6. [PubMed: 19136488]
3. Ding J, Hsu FC, Harris TB, et al. The association of pericardial fat with incident coronary heart disease: the Multi-Ethnic Study of Atherosclerosis (MESA). Am J Clin Nutr. 2009; 90:499–504. [PubMed: 19571212]
4. Shimokawa H, Ito A, Fukumoto Y, et al. Chronic treatment with interleukin-1 beta induces coronary intimal lesions and vasospastic responses in pigs in vivo. The role of platelet-derived growth factor. J Clin Invest. 1996; 97:769–76. [PubMed: 8609234]
5. Gorter PM, van Lindert AS, de Vos AM, et al. Quantification of epicardial and peri-coronary fat using cardiac computed tomography; reproducibility and relation with obesity and metabolic syndrome in patients suspected of coronary artery disease. Atherosclerosis. 2008; 197:896–903. [PubMed: 17884060]
6. Mazurek T, Zhang L, Zalewski A, et al. Human epicardial adipose tissue is a source of inflammatory mediators. Circulation. 2003; 108:2460–6. [PubMed: 14581396]
7. Gorter PM, de Vos AM, van der Graaf Y, et al. Relation of epicardial and pericoronary fat to coronary atherosclerosis and coronary artery calcium in patients undergoing coronary angiography. Am J Cardiol. 2008; 102:380–5. [PubMed: 18678291]
8. de Vos AM, Prokop M, Roos CJ, et al. Peri-coronary epicardial adipose tissue is related to cardiovascular risk factors and coronary artery calcification in post-menopausal women. Eur Heart J. 2008; 29:777–83. [PubMed: 18156138]
9. Mahabadi AA, Reinsch N, Lehmann N, et al. Association of pericoronary fat volume with atherosclerotic plaque burden in the underlying coronary artery: a segment analysis. Atherosclerosis. 2010; 211:195–9. [PubMed: 20223460]
10. Libby P, Ridker PM, Hansson GK. Inflammation in atherosclerosis: from pathophysiology to practice. J Am Coll Cardiol. 2009; 54:2129–38. [PubMed: 19942084]
11. Ridker PM, Cannon CP, Morrow D, et al. C-reactive protein levels and outcomes after statin therapy. N Engl J Med. 2005; 352:20–8. [PubMed: 15635109]
12. Ridker PM, Danielson E, Fonseca FA, et al. Rosuvastatin to prevent vascular events in men and women with elevated C-reactive protein. N Engl J Med. 2008; 359:2195–207. [PubMed: 18997196]
13. Mora S, Ridker PM. Justification for the Use of Statins in Primary Prevention: an Intervention Trial Evaluating Rosuvastatin (JUPITER)--can C-reactive protein be used to target statin therapy in primary prevention? Am J Cardiol. 2006; 97:33A–41A.
14. Fortmann SP, Ford E, Criqui MH, et al. CDC/AHA Workshop on Markers of Inflammation and Cardiovascular Disease: Application to Clinical and Public Health Practice: report from the population science discussion group. Circulation. 2004; 110:e554–9. [PubMed: 15611381]
15. Hoffmann U, Bamberg F, Chae CU, et al. Coronary computed tomography angiography for early triage of patients with acute chest pain: the ROMICAT (Rule Out Myocardial Infarction using Computer Assisted Tomography) trial. J Am Coll Cardiol. 2009; 53:1642–50. [PubMed: 19406338]
16. Pearson TA, Mensah GA, Alexander RW, et al. Markers of inflammation and cardiovascular disease: application to clinical and public health practice: A statement for healthcare professionals from the Centers for Disease Control and Prevention and the American Heart Association. Circulation. 2003; 107:499–511. [PubMed: 12551878]
17. Austen WG, Edwards JE, Frye RL, et al. A reporting system on patients evaluated for coronary artery disease. Report of the Ad Hoc Committee for Grading of Coronary Artery Disease, Council on Cardiovascular Surgery. American Heart Association Circulation. 1975; 51:5–40.

18. Bamberg F, Dannemann N, Shapiro MD, et al. Association between cardiovascular risk profiles and the presence and extent of different types of coronary atherosclerotic plaque as detected by multidetector computed tomography. Arterioscler Thromb Vasc Biol. 2008; 28:568–74. [PubMed: 18174458]

19. Blackmon KN, Streck J, Thilo C, Bastarrika G, Costello P, Joseph Schoepf U. Reproducibility of automated noncalcified coronary artery plaque burden assessment at coronary CT angiography. J Thorac Imaging. 2009; 24:96–102. [PubMed: 19465831]

20. Lehman SJ, Schlett CL, Bamberg F, et al. Assessment of coronary plaque progression in coronary computed tomography angiography using a semiquantitative score. JACC Cardiovasc Imaging. 2009; 2:1262–70. [PubMed: 19909929]

21. Djaberi R, Schuijf JD, van Werkhoven JM, Nucifora G, Jukema JW, Bax JJ. Relation of epicardial adipose tissue to coronary atherosclerosis. Am J Cardiol. 2008; 102:1602–7. [PubMed: 19064012]

22. Maurovich-Horvat P, Massaro J, Fox CS, Moselewski F, O'Donnell CJ, Hoffmann U. Comparison of anthropometric, area- and volume-based assessment of abdominal subcutaneous and visceral adipose tissue volumes using multi-detector computed tomography. Int J Obes (Lond). 2007; 31:500–6. [PubMed: 16953256]

23. Abbara S, Desai JC, Cury RC, Butler J, Nieman K, Reddy V. Mapping epicardial fat with multi-detector computed tomography to facilitate percutaneous transepicardial arrhythmia ablation. Eur J Radiol. 2006; 57:417–22. [PubMed: 16434161]

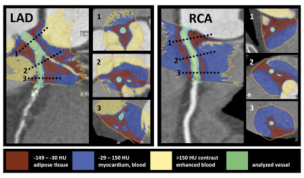

Figure 1.

Threshold based volumetric pericoronary adipose tissue quantification (left panel: LAD, right panel: RCA). The inserted cross-sections correspond to levels marked with dotted lines on the LAD and RCA. The manual tracing (yellow line) of the region of interest is performed on muliplanar-reformatted images perpendicular to the vessel centerline. The voxels within the predefined Hounsfield unit range are summarized, and the adipose tissue volume is calculated automatically. The red color indicates fat containing voxels. The blue color indicates the vessel wall, myocardium, and the non-enhanced blood pool. The yellow color indicates the contrast enhanced blood filled lumen and cavities. The green color indicates the analyzed vessel.

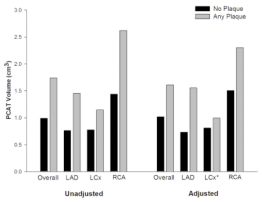

Figure 2.

Mean PCAT volume surrounding subsegments with coronary plaque versus no plaque for each coronary vessel separately and all three vessels combined (overall). Adjusted analyses performed using mixed effects modeling, accounting for the matched pairs, individual patient estimates, and adjusted for vessel, distance, BMI, hypertension, hyperlipidemia, and hs-CRP. All p values < 0.001, except for * where p=0.14.

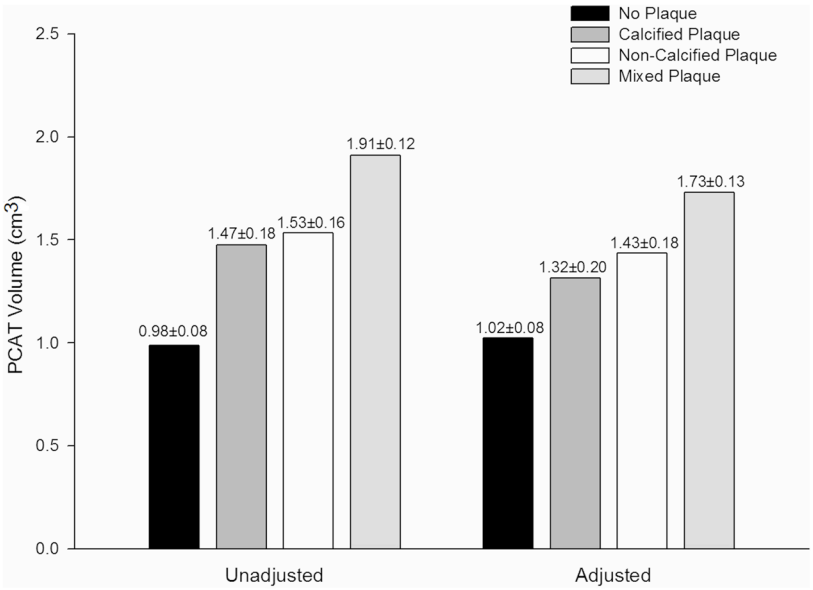

Figure 3.

Mean PCAT volume ± standard error based on Plaque Morphology. Adjusted analyses performed using mixed effects modeling, accounting for the matched pairs, individual patient estimates, and adjusted for vessel, distance, BMI, hypertension, hyperlipidemia, and hs-CRP. The p-values for the mixed model overall were <0.001 for both adjusted and unadjusted analyses.

Table 1

Demographics of overall cohort and matched groups

	Overall (n = 51)	Group 1 Plaque, hs-CRP>2 (n = 17)	Group 2 No plaque, hs-CRP>2 (n = 17)	Group 3 No plaque, hs-CRP<1 (n = 17)	p
Demographics					
Age (years)	49.5 ± 5.1	49.9 ± 5.5	49.0 ± 5.2	49.8 ± 4.9	0.87
Male	33 (65%)	11 (65%)	11 (65%)	11 (65%)	1.0
Caucasian	44 (86%)	15 (88%)	14 (82%)	15 (88%)	1.0
BMI (kg/m^2)	28.5 ± 4.9	29.1 ± 4.2	30.3 ± 6.2	26.3 ± 3.2	0.05
Risk factors					
Diabetes	4 (8%)	3 (178%)	0 (0)	1 (6%)	0.31
Hypertension	14 (27%)	8 (47%)	4 (24%)	2 (12%)	0.09
Hyperlipidemia	15 (29%)	10 (58%)	2 (12%)	3 (18%)	0.01
Smoking	29 (57%)	12 (71%)	8 (47%)	9 (53%)	0.46
Family history of CAD	37 (73%)	13 (76%)	11 (65%)	13 (76)	0.79
Framingham Risk Score					
Low (<10%)	38 (76%)	13 (76%)	13 (76%)	12 (75%)	
Intermediate (0–20%)	10 (20%)	2 (12%)	4 (24%)	4 (25%)	0.44
High (>20%)	2 (4%)	2 (12%)	0 (0%)	0 (0%)	
Presenting symptoms/vital signs					
Chest pain duration (min) [IQR]	90 [15–180]	45 [11–180]	120 [15–210]	120 [20–180]	0.32
Systolic blood pressure (mmHg)	133 ± 18	127 ± 15	137 ± 19	134 ±18	0.25
Diastolic blood pressure (mmHg)	79 ± 13	74 ± 12	82 ± 14	80 ± 12	0.16
Heart rate (bpm)	78.1±17.5	77.1±15.6	80.2 ±10.7	77.2 ± 24.4	0.85
Medications on presentation					
Aspirin	12 (24%)	4 (24%)	6 (35%)	2 (12%)	0.33
Beta-blockers	5 (10%)	4 (24%)	0 (0%)	1 (6%)	0.11
Statins	9 (18%)	6 (35%)	1 (6%)	2 (12%)	0.11
ACE-I	5 (10%)	4 (24%)	0 0%)	1 (6%)	0.11
Laboratory tests					

	Overall (n = 51)	Group 1 Plaque, hs-CRP>2 (n = 17)	Group 2 No plaque, hs-CRP>2 (n = 17)	Group 3 No plaque, hs-CRP<1 (n = 17)	p
hs-CRP (mg/L) [IQR]	2.62 [0.63–3.69]	3.86 [3.16–8.75]	2.88 [2.41–3.65]	0.39 [0.32–0.63]	<0.0001
hs-CRP > 2 mg/L	34 (67%)	17 (100%)	17 (100%)	0 (0%)	<0.0001
GFR (ml/min/1.73m^2)	86.3 ± 13.2	90.0 ± 15.5	84.2 ± 14.0	84.6 ± 9.3	0.36

BMI denotes body mass index; CAD, coronary artery disease; IQR, interquartile range; ACE-I, angiotensin converting enzyme inhibitor; hs-CRP, high sensitivity C-reactive protein; and GFR, glomerular filtration rate.

Table 2

Intra- and inter- observer reproducibility of PCAT measurement

PCAT Volumes	Intra-observer			Inter-observer		
	Mean Actual Difference(cm^3)	Percent Difference	ICC	Mean Actual Difference(cm^3)	Percent Difference	ICC
Proximal 40 mm distance						
All coronaries	0.27 ± 0.91	0.61%	0.997	1.38 ± 3.32	3.00%	0.951
LAD	0.0 ± 0.25	0.14%	0.995	0.32 ± 1.02	1.15%	0.876
LCx	0.16 ± 0.55	1.47%	0.987	0.69 ± 2.20	5.22%	0.791
RCA	0.16 ±0.52	0.21%	0.997	0.37 ± 1.21	2.25%	0.982
Entire Vessel length						
All coronaries	4.53 ± 15.27	7.71%	0.804	28.39 ± 17.29†	29.73%	0.405
LAD	1.06 ± 7.38	5.64%	0.667	6.45 ± 5.60†	20.63%	0.511
LCx	4.03 ± 9.93	36.11%	0.209*	8.21 ± 9.10	35.83%	0.181*
RCA	0.56 ± 10.52	1.94%	0.708	13.74 ± 10.58†	30.56%	0.395
Proximal anatomical segments						
All coronaries	3.47 ± 3.33†	19.89%	0.891	5.32 ± 4.05†	32.22%	0.802
LAD	0.53 ± 0.87	12.23%	0.937	0.13 ± 1.47	1.77%	0.901
LCx	0.11 ± 2.09	3.61%	0.365*	0.64 ± 1.64	3.58%	0.381*
RCA	1.02 ± 2.66	11.27%	0.887	3.88 ± 2.62†	30.04%	0.688
Proximal two anatomical segments						
All coronaries	23.09 ± 20.0†	47.90%	0.378	19.63 ± 12.52†	39.31%	0.670
LAD	0.73 ± 0.77†	9.80%	0.956	0.91 ± 3.87	3.55%	0.603
LCx	4.03 ± 10.0	36.11%	0.209*	8.69 ± 9.10†	40.36%	0.175*
RCA	0.85 ± 7.04	4.25%	0.740	6.53 ± 4.17†	21.70%	0.596

Intra-observer and inter-observer reproducibility of each measure were reported as ICC with all $p<0.05$, except for *p=nonsignificant. All p-values for the mean actual difference were nonsignificant except for †$p \leq 0.01$.

Proximal anatomical segments includes only segments 1, 5, 6, and 11. Proximal two anatomical segments include only segments 1, 2, 5, 6, 7, 11 and 13. LAD denotes left anterior descending artery; LCx, left circumflex artery; RCA, right coronary artery; ICC, intraclass correlation coefficient.

Table 3

Patient and vessel based analysis and PCAT measures

PCAT Volume (cm^3)	Any Plaque hs-CRP >2	No Plaque, hs-CRP >2	No Plaque, hs-CRP <1	p value
All coronaries	39.65 ± 2.67	22.37 ± 2.90	24.72 ± 3.42	< 0.001
LAD*	10.50 ± 1.05	5.83 ± 1.03	5.82 ± 1.33	0.003
LCx	9.55 ± 0.99	6.49 ± 0.91	6.00 ± 1.16	0.039
RCA	18.21 ± 1.60	14.24 ± 1.46	13.11± 1.90	0.051

Values are reported as mean ± standard error. PCAT denotes pericoronary adipose tissue, hs-CRP, high sensitivity C-reactive protein; LAD, left anterior descending artery; LCx, left circumflex artery; RCA, right coronary artery. All mixed effect models were accounted for the matching performed and are adjusted for BMI, hypertension, and hyperlipidemia.

* Indicates that a non-parametric model was used to generate the p-value.